Structural investigations in (Al)-ZSM-12 with MTEA or TEA cations

Marta Počkaj[a] , Anton Meden[a], Nataša Zabukovec Logar[b,c], Mojca Rangus[b], Ines Lezcano-Gonzalez[d,e], Andrew M. Beale[d,e] and Amalija Golobič[a, *]

[a]*Faculty of Chemistry and Chemical Technology, University of Ljubljana, Večna pot 113, 1000 Ljubljana, Slovenia;*

[b]*National Institute of Chemistry, Hajdrihova 19, 1000 Ljubljana, Slovenia;*

[c]*University of Nova Gorica, Vipavska 13, 5000 Nova Gorica, Slovenia;*

[d]*Research Complex at Harwell, Rutherford Appleton Laboratories, Harwell Science and Innovation Campus, Harwell, Didcot, Oxon, OX11 0FA, UK*

[e]*Department of Chemistry, University College London, 20 Gordon Street, London, WC1H 0AJ, UK*

[*]Corresponding author; *E-mail:amalija.golobic@fkkt.uni-lj.si.*

Abstract

Two different quaternary ammonium cations, methyltriethyl- (MTEA) and tetraethylammonium cations (TEA) were used as templates in the synthesis of pure-silica as well as aluminosilicate ZSM-12 (MTW-type) frameworks. The distribution of the template cations in the 12MR channels in the 1-dimensional framework topology was studied; thus the as-prepared products were characterized by means of X-ray powder diffraction, Raman, transmission FTIR, solid-state NMR spectroscopy, thermogravimetric and elemental analyses and SEM. Recently, it was shown that in pure-silica (PS) ZSM-12, TEA cations are well ordered - a superstructure with three-times longer *b* edge along the channel is formed, which can be seen by virtue of a few additional peaks in the X-ray powder pattern. Herein we describe that its aluminosilicate counterpart with TEA also contains ordered TEA cations and is isostructural to PS-ZSM-12. Conversely, in both pure-silica and aluminosilicate ZSM-12 frameworks with MTEA, the cations are disordered and no superstructure is formed.

d. Keywords: zeolite, ZSM-12; TEA; MTEA; superstructure; X-ray powder diffraction.

1. Introduction

Zeolite ZSM-12 (MTW framework type) belongs to the family of 1-dimensional zeolites with 12-membered rings which run along the *b*-edge. Although not commonly used for industrial purposes, it shows potential for use as a catalyst at different processes in petrochemical industry, e.g. cracking, hydrocracking, different alkylations and isomerisations [1]. The fundamental properties of the framework comprise the following: unit cell parameters, a=25.552, b=5.256, c=12.117 Å, β=109.312°,

V=1535.78 Å^3, space group *C*2/*m* [2, 3]. The framework topology was first determined by LaPierre and co-workers [4] using a combination of electron and X-ray diffraction with model building leading to *C*2/*m* cell with parameters *a*=24.88(4), *b*=5.02(2), *c*=12.15(3) Å, *β*=107.7(1)° and seven symmetrically independent silicon atoms, confirmed by the ^{29}Si NMR study of Trewella *et al*. [5]. Additional studies, especially combinations of complementary synchrotron XRD and NMR, further confirmed the *C*2/*c* framework symmetry. In this case, the unit cell is doubled along *c* axis, yielding *a*=24.8633(3), *b*=5.01238(7), *c*=24.3275(7) Å, *β*=107.7215(6)° [6].

To date, ZSM-12 can be prepared in the presence of several different organic cations (organic structure directing agents, OSDA), most of which are quaternary ammonium cations. A few reports on OSDA-free synthesis of ZSM-12 are also available [7,8]. The most frequently used OSDA is the tetraethylammonium cation (TEA). Recently, we discovered that TEA cations order in the ZSM-12 channels and consequently, a superstructure with a three times larger unit cell is formed [9]. However, a few questions remain unanswered; firstly, does the inclusion of Al^{3+} in the zeolite framework affect the ordering of the TEA cations? If so, what is the highest concentration of Al^{3+} that enables the formation of the superstructure?

On the other hand, methyltriethylammonium cations (MTEA) are of a similar size with similar physico-chemical characteristics as TEA and it also enables the formation of MTW framework [10]. The question here is, whether MTEA cations also order in the channels of ZSM-12 or not? Therefore, the aim of this study was to explore the

presence of ordering of TEA and MTEA cations when trapped in the zeolite channels of pure-silica and aluminium-containing ZSM-12, respectively.

2. Experimental

2.1. Synthesis

Pure-silica ZSM-12 with MTEA was prepared according to a modified double-silica source method published by Mitra *et al.* [11]. The molar ratio between reactants was as follows: 1 Na_2SiO_3: 147 H_2O : 3.80 MTEAOH : 12.50 SiO_2. Initially, 0.325 g (2.67 mmol) of Na_2SiO_3 was dissolved in distilled water (1.75 g, 0.097 mol), followed by dropwise addition of 6.67 g of MTEAOH (20 %, Sigma Aldrich) to the clear solution. The mixture was allowed to stir at room temperature for 0.5 h and then, 2.00 g of SiO_2 was added (Davisil, mesh size 35−60, 150 Å, Sigma Aldrich). After additional stirring for 3.5 h, the obtained highly alkaline gel was transferred to teflon-lined stainless steel autoclaves (~20 mL) and heated for 1−8 days at 150 °C under static conditions. When the reaction finished, the products were filtered off, washed with distilled water to neutral pH value and dried at 50 °C overnight.

Al-ZSM-12 with TEA or MTEA, respectively, were prepared by the modified synthethic route as published by Gopal *et al.* [12]. In case of TEA, the molar ratios between the reactants were *x* Na_2O : *x* Al_2O_3 : 80 SiO_2 : 12.7 TEAOH : 1040 H_2O, where *x* = 0.25, 0.50, 0.57, 0.67, 0.80, 1.00, 1.33 and 2.00 (representing Si : Al molar ratios of 160, 80, 70, 60, 50, 40, 30 and 20, respectively). In case of MTEA, the molar ratios were 1 Na_2O : 1 Al_2O_3 : 80 SiO_2 : 12.5 MTEAOH : 980 H_2O (*i.e.* Si : Al = 40). Initially, appropriate amounts of MTEAOH or TEAOH (35 wt. %, Sigma Aldrich) were

diluted with distilled water, followed by the slow addition of $NaAlO_2$ (Alfa Aesar, technical grade). When the solid was dissolved, Ludox HS-40 (Sigma Aldrich) was added dropwise and stirred for a few minutes. The obtained gel with low viscosity was then transferred to teflon-lined stainless steel autoclaves and heated at 150 °C under static conditions for 3−8 days. The solid products were isolated from the highly basic reaction mixture, washed with distilled water to neutral pH value and dried at 50 °C overnight.

2.2. Characterization methods

X-ray powder diffraction data were collected using a PANalytical X'Pert PRO MPD diffractometer with reflection geometry and primary side Johansson type monochromator, with $CuK_{\alpha 1}$ wavelength (1.540596 Å). Rietveld refinement was performed with TOPAS Academic software [13] on the product obtained with a Si:Al ratio of 80 and heating time of 96 hours. The crystal data, collection conditions and refinement parameters are presented in Table 1.

The compositional weight percentage of carbon, hydrogen and nitrogen were determined on Perkin Elmer 2400 CHN microanaliser by the Chemistry Department service at the University of Ljubljana. The weight per cent of silicon and aluminum in the products were estimated using an inductively coupled plasma-atomic emission spectrometer (ICP-AES, Thermo Jarrell Ash, model Atomscan 25 with ultrasonic nebulizer Cetac, model U-6000 AT) at National Institute of Chemistry, Ljubljana.

Raman spectra were recorded on a Holoprobe Kaiser Optical spectrometer. The spectrometer makes use of a Nd:YAG laser source which operates at a wavelength of

532 nm (frequency doubled) with a typical power output of 60 mW. A CCD camera was used for signal detection through a pair of holographic notch filters. A 1.3" objective lense was used to focus the laser light. The sample was first pressed into a disc-shaped, self-supporting wafer before measurements were performed with a collection time of 2 s per spectra. In order to improve the signal-to-noise statistics, 240 spectra were recorded and summed.

FTIR measurements were performed on self-supporting wafers of the as-prepared zeolite materials (0.01 to 0.02 g) using a Perkin Elmer 2000 spectrometer (25 scans were collected per measurement over a range of 4000–1300 cm^{-1} with a resolution of 4 cm^{-1}). The wafer was placed in an IR transmission cell equipped with CaF_2 windows. The cell was first evacuated to $2 \cdot 10^{-8}$ bar before the temperature was raised from 323 K to 573 K at 3 K/min and held for 2 h in order to dehydrate the sample.

Thermal analysis of the product (TG/DTG) was performed on a SDT 2960 Thermal Analysis System (TA Instruments, Inc.). The measurements were carried out under nitrogen flow with a heating rate of 10 °C/min up to 720 °C.

Solid-state ^{27}Al MAS, ^{1}H-^{29}Si CPMAS and ^{29}Si MAS NMR spectra were recorded on a 600 MHz (14.1 T) Varian VNMRS spectrometer using a Varian 3.2 mm double resonance MAS probe. Solid samples were spun at 10 kHz for ^{29}Si and 16 kHz for ^{27}Al MAS spectra. A single-pulse excitation with repetition delays of 0.5 s and 30 s, and 15,000 and 1,500 scans accumulated for ^{27}Al and ^{29}Si nuclei was used, respectively. For the ^{1}H-^{29}Si CPMAS acquisition, a repetition delay of 5 s was adopted and 4000 scans

were accumulated. The ^{27}Al spectra were referenced to $Al(NO_3)_3$, while the ^{29}Si spectra were referenced to 2,2-dimethyl-2-silanpentane-5-sulphonic acid (DSS), with a chemical shift of $\delta = 1.53$ ppm relative to tetramethylsilane (TMS).The morphology of the samples was studied by Zeiss ULTRA 55 plus field-emmission scanning electron microscope (FE-SEM). A small quantity of powder sample was placed onto the sample holder and coated with gold to obtain appropriate conductivity.

3. Results and Discussion

3.1. Al-ZSM-12 with TEA

3.1.1. Characterization of the framework

ZSM-12 is a representative of high-silica zeolites. For almost a decade, the lowest achieved molar ratio Si:Al was ~ 30 [12], i.e. the highest achievable mass per cent of Al^{3+} in a calcined framework was believed to be ~ 1.5 %. Further modification of the synthesis conditions (e.g. different source of Al, SiO_2 and OSDA) led to lower Si:Al ratios were obtained: 10.4–14.6 by Kamimura *et al*. using an OSDA-free synthesis approach [7] and ~12 by Paris *et al*. by employing of combination of organic and inorganic structure directing agents [14]. Currently, the richest reported Al-ZSM-12 has a Si:Al ratio of 8–23, prepared with the assisstance of N,N,N′,N′-tetraethylbicyclo[2.2.2]oct-7-ene-2,3:5,6-dipyrrolidinium cation [15]. In our syntheses, the Si:Al molar ratios range from 20 to 160. Figure 1a shows the powder patterns of the as-prepared Al-ZSM-12 products with TEA cations; for comparison, the powder pattern of highly crystalline PS-ZSM-12 with TEA is also given. It can be clearly seen that for

Si:Al ≥ 40, the MTW framework with occluded template and without any other crystalline impurity is formed. In contrast, amorphous products are obtained for lower Si:Al ratios. As in PS-ZSM-12 with TEA, weak superstructural diffraction peaks that indicate the formation of superstructure can be observed in all samples (Fig. 1b). These are less pronounced due to the lower crystallinity (i.e. wider diffraction peaks) of the Al-ZSM-12 with TEA in comparison with pure-silica analogue.

Insert FIG. 1

To prove the incorporation of aluminum into the framework, other techniques including scanning electron microscopy, elemental analysis (ICP-AES) and solid-state NMR spectroscopy were used. Namely, the diffraction peaks are quite broad and their positions cannot be determined very precisely – even if the size difference were significant, the lower crystallinity/smaller particle size of the Al-ZSM-12 samples would not allow us to determine whether the larger Al^{3+} ion is incorporated into the framework.

The SEM images provide the first evidence of the inclusion of Al into the zeolite framework. It is well-known that the crystallinity of the high-silica zeolites drops rapidly with the presence of aluminum in the reaction mixture [16]. In our case the crystal grains of Al-containing products are much smaller in comparison with the pure-silica product (Fig. 2): here the edges of the intergrown cubes are several nm long while in the pure-silica product the polyhedral grains are several micrometers long.

Insert FIG. 2

However, different reaction conditions (i.e. different Si source) can also lead to ZSM-12 crystals possessing a smaller particle size and so additional characterization methods

(ICP-AES, NMR) that would provide evidence for the incorporation of Al into the framework were also used. The results of elemental analysis presented in Table 2 show that Si:Al ratio in the product is slightly lower in comparison with the , i.e. the tendency of Al to include into the framework is higher in comparison with Si. It seems that Al incorporates rapidly into the crystallization nuclei which become negatively charged leading to a stronger interaction between the crystal nuclei and cationic template [17]. With increased Al concentration, crystal nuclei formation prevails over subsequent crystal growth.

In the ^{27}Al NMR spectrum of Al-ZSM-12 TEA (Fig. 3) a single resonance peak at the chemical shift of 53.2 ppm can be observed, which belongs to the 4-fold coordinated Al^{3+} atoms [18]. Similar ^{27}Al chemical shifts were observed for ZSM-12 samples prepared with TEAOH and TEABr templates [19]. No resonances in the regions indicative of five-fold and octahedrally coordinated Al atoms were observed. Note however, that the relatively broad signal around 0 ppm denoted with an asterisk (Figure 3) is due to the rotor background. The presence of only four-fold coordinated Al atoms in the ZSM-12 TEA sample confirms that all aluminum atoms are incorporated in the zeolite framework. The results are consistent with earlier studies of Al-ZSM-12 with TEA, where the presence of extra-framework Al was also not observed [20]. The quantitative phase determination by Rietveld refinement using a standard addition method was performed revealing a small amount of amorphous phase (~ 3%; details are given in Supplementary material).

Insert FIG. 3

For pure or high silica, highly crystalline zeolite samples, solid-state ^{29}Si MAS NMR can distinguish between signals originating form crystallographicaly inequivalent T sites [6, 21, 22, 23]. However, when dealing with a sample with a higher degree of disorder, resonance lines get broadened and consequently individual contributions cannot be resolved. This also happens in our case: both PS and Al-ZSM-12 samples were synthesized in strong basic media leading to a high concentration of defective silanol groups (*vide infra*), so the materials were not crystalline enough to spot the contributions of individual crystallographic sites of Si atoms (see Suppl. material, Fig. S-1). Consequently, for Al-ZSM-12 we presumed that Si atoms occuppy the same sites as in PS-ZSM-12, and according to elemental analysis, we adjusted the occupancies of all T-sites between Al and Si to get the expected composition.

In PS-ZSM-12 framework, SiO^- groups are required to neutralize the positive charge of TEA cations. When introducing Al into the framework, the latter gets negatively charged but due to a small amount of Al, siloxy defects may be still necessary to obtain the electroneutral structure. As seen in Fig. 4, the IR spectrum of Al-ZSM-12 with TEA recorded under vacuum at 523 K exhibits the characteristic spectral features due to the TEA cation, including C−H deformation (1455 and 1483 cm^{-1}) and C−H stretch modes (2954 and 2986 cm^{-1}) of the ethyl groups [9], together with peaks at ~3735 and 3690 cm^{-1}, resulting from the presence of isolated and hydrogen-bonded/vicinal silanol groups, respectively [24]. No Si−O^-...HO−Si groups could be detected – typically giving a broad signal at about 3200 cm^{-1}, probably due to their conversion into silanol groups during the thermal treatment as the organic cations start to decompose [9].

Insert FIG. 4

3.1.2. Characterization of TEA cations

The quantity of organic template in the Al-ZSM-12 framework was determined by elemental CHN and thermogravimetric analyses. As presented in Table 3, experimentally obtained values for the sample containing Si:Al = 80 (96 h, 150 °C) are in good agreement with the calculated ones. For the calculation we expected the presence of two TEA cations in a cell three times larger when compared to the original ZSM-12 framework [6] (just as in pure-silica ZSM-12 with TEA), and molar ratio Si:Al 70:1 (see Table 2). The total amount of organic cations from CHN analysis is comparable to the mass loss in TG curve (Fig. 5). The first mass loss step includes the evaporation of adsorbed water (until ~120 °C, 1,58 %). Between ~120 and 500 °C, organic cations from the framework is lost (10,16 % of initial mass). The last, almost imperceptible, mass loss step arises from water condensation from framework silanol groups which most likely occurs at the same time as the decomposition of organic cations.

Insert FIG. 5

As TEA cations appear predominantly in two conformer states [25] it was necessary to find out the prevailent conformer state in the studied compound. As in the PS analogue, the results from Raman spectroscopy show only the presence of one conformer state *tt.tt* conformer (C_4N stretching at 676 cm^{-1}, Fig. S-2) [26].

3.1.3. Structural characterization of Al-ZSM-12 with TEA

As the initial structural model for Rietveld refinement, the structure of PS-ZSM-12 with TEA was used. For structural analysis, the sample with Si:Al synthetic ratio 80 was used. The occupancies of the tetrahedral sites were adjusted to be in agreement with the

results of elemental analysis, i.e. 0.986 for Si and 0.014 for Al. At first, a trial was made to adapt the framework to the fixed cation positions. Although a large number of geometry constraints were used, the resulting framework always possesed either unacceptably long Si−O bonds or Si−O−Si angles that deviated from the values recommended by Wragg and co-workers [27], or too short contact distances between TEA cations and the framework. We also attempted the opposite, i.e. trying to find the optimal cation positions for a fixed framework. Again, the obtained results were not acceptable due to unfavourable packing of cations (too long or too short distances between the neighbouring ones and/or too short contacts between TEA and the framework).

The decision was taken to fix the framework and cation atoms positions and refine 18 independent parameters: scale factor, zero error, 6 parameters for background description, 4 profile parameters, 4 unit cell parameters and 2 displacement parameters (for tetrahedral and oxygen atoms, respectively). The crystal structure changed only slightly; due to the lower crystallinity of Al-ZSM-12 the unit cell parameters are less accurately determined as in pure-silica ZSM-12. The final Rietveld plot can be seen in Fig. 6, and the crystal data, collection conditions and refinement parameters are presented in Table 1.

Insert FIG. 6

Insert Table 1

3.2. ZSM-12 and Al-ZSM-12 with MTEA

Template cations TEA and MTEA differ only in the presence of one methyl group, possessing similar chemical features and size, so MTEA should enable the formation of MTW framework. One would expect that MTEA cations order in the zeolite channels and thus form the superstructure as in the TEA case, although the smaller MTEA molecule has been previously considered a pore-filling rather than a structure directing agent [10]. However, no superstructural peaks are present in the powder patterns of PS ZSM-12 nor Al-ZSM-12 with MTEA irrespective of synthesis conditions such as heating time and temperature (Fig. 7). TG and CHN analyses of both samples with MTEA have shown the presence of approximately 2/3 of MTEA cations per unit cell (*b* ~ 5 Å) which is expected and compatible with the cationic size and minimal contact distances according to the relevant van der Waals radii. The inclusion of MTEA in the framework channels and the negative charge of the framework were also proven by the FTIR measurements, showing the same features as pure-silica and Al-ZSM-12 with TEA.

Insert FIG. 7

An interesting difference between ZSM-12 with TEA or MTEA can be observed from their SEM images. Rather larger crystallites grow from the reaction mixtures containing MTEA (Fig. 8), and no significant differences in crystallinity are seen between the pure-silica and aluminosilicate samples –in contrast to the results obtained in the presence of TEA (cf. Fig. 2) and indicating a different role and mechanism of growth caused by one or another cation.

Insert FIG. 8

^{27}Al MAS NMR spectrum of the ZSM-12 with MTEA (Figure 3) similarly exhibits a single resonance peak at 56 ppm which can be, as in the case of Al-ZSM-12 with TEA, assigned to tetrahedrally coordinated aluminium in the zeolite framework. No additional resonances at 0 ppm, belonging to extra-framework Al species, were observed.

4. Conclusions

Pure-silica as well as aluminosilicate ZSM-12 frameworks were prepared with assistance of TEA and MTEA cations. The results of standard physico-chemical characterization techniques have shown that TEA cations order in aluminosilicate ZSM-12 framework in the same manner as in pure-silica ZSM-12 [9]. Namely, in the powder patterns of both zeolites, a few additional weak superstructural peaks appear revealing a superstructure with three-times longer *b* edge along the channels. This accounts for the additional peaks seen in the XRD data i.e.; they do not belong to any impurities. By means of Rietveld refinement on conventional laboratory powder data the crystal structure of Al-ZSM-12 with TEA was established. With MTEA cations however, the situation is rather different, and these are disordered in pure-silica and also in aluminosilicate ZSM-12.

5. Appendices

5.1. Amorphous phase content calculation (method of standard addition)

The amorphous phase content in the Al-ZSM-12 sample with TEA (synthesis ratio Si:Al = 80) was calculated by standard addition method of corundum (Al_2O_3), based on powder diffraction data, by equation

w(amorphous phase) = 1– ($w_{corundum,\ true}/w_{corundum,Rietveld}$).

A known mass of Al_2O_3 (25.8 mg) was added to the Al-ZSM-12 with TEA sample (79.2 mg), being the true weight fraction of Al_2O_3 ($w_{corundum,\ true}$) 0.246. Rietveld method gave a mass fraction of Al_2O_3 of 0.253 ($w_{corundum,Rietveld}$). Accordingly, the estimated mass per cent of amorphous phase in the original sample of Al-ZSM-12 with TEA is ~2.8%.

5.2. Supplementary figures

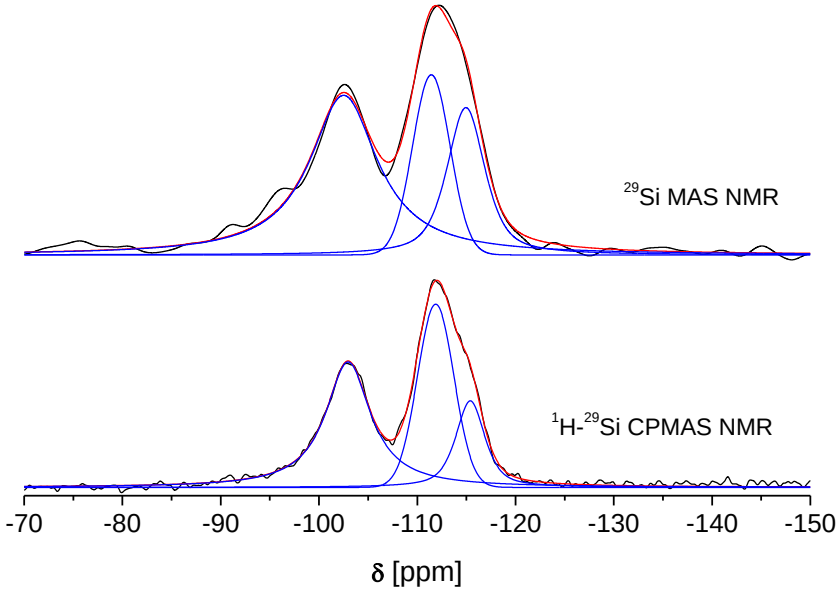

Fig. S-1A. ^{29}Si MAS and ^{1}H-^{29}Si CPMAS NMR spectra of PS-ZSM-12 (black lines), their decomposition into individual contributions (blue lines) and the best fit (red lines). The analyses indicate that three different Si environments can be observed.

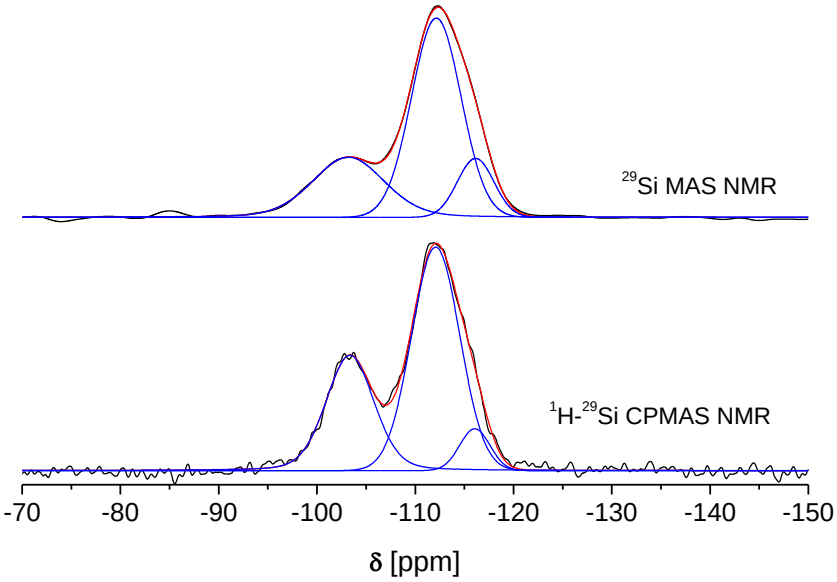

Fig. S-1B. ^{29}Si MAS and ^{1}H-^{29}Si CPMAS NMR spectra of Al-ZSM-12 with TEA (Si:Al = 80, 96 h, 150 °C) (black lines), their decomposition into individual contributions (blue lines) and the best fit (red lines). The analyses indicate that three different Si environments can be observed.

The ^{29}Si NMR spectra of the pure siliceous zeolite (Figure S-1) show three individual silicon resonances. The two resonances at –115 and –112 ppm can be readily attributed to the presence of $Si(OSi)_4$ environments (47 %). The additional signal at a lower field (–103 ppm) indicates a presence of structural defect groups of $Si(OSi)_3OH$ type (53 %) [17, 28]. Similarly, in the case of Al-containing ZSM-12 with TEA (Si:Al = 80) (Figure S-2) three individual contributions can be distinguished, the ones at –116 and –112 ppm belonging to $Si(OSi)_4$ (72 %) and the peak at –103 ppm to $Si(OSi)_3OH$ silicon species (28 %). The high Si:Al ratio of the sample makes the intensity of the signal belonging to Si(3Si,1Al) environments, which also resonate at frequencies around –103 ppm, only about 5 % of all Si(4Si,0Al) signals. This and the fact that intensity of the –103 ppm resonance is enhanced in the ^{1}H-^{29}Si CPMAS spectrum points to the majority of this

signal originates from $Si(OSi)_3OH$ species. In comparison to pure siliceous zeolite Al-ZSM-12 with TEA exhibits far less structural defects. Since ^{1}H-^{29}Si CPMAS spectra show no resonances at fields lower than –103 ppm, the structural defects of the and $Si(OSi)_2(OH)_2$ type can be excluded.

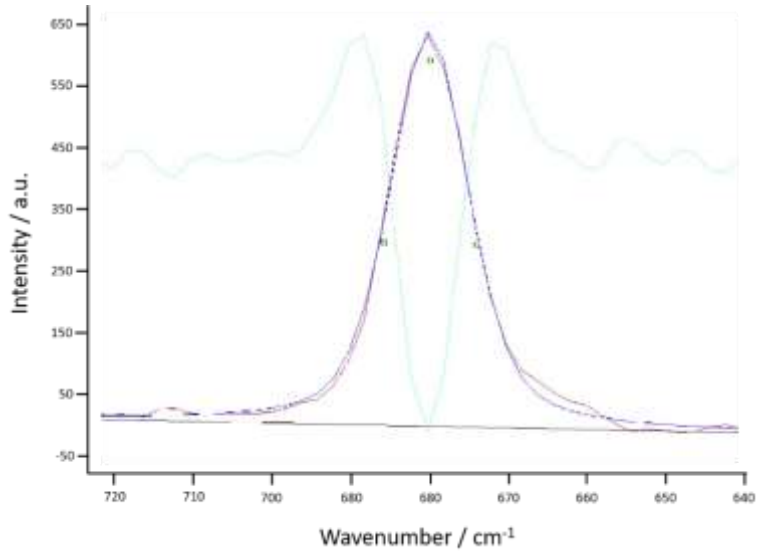

Fig. S-2. Raman spectrum of Al-ZSM-12 with TEA (Si:Al ratio 80); in the displayed section a differentiation between both rotamers of TEA cations is possible. Here the presence of tt.tt rotamer is confirmed. Red curve presents measured, blue calculated profile and cyan a second derivative of the measured curve.

6. Acknowledgements

The authors acknowledge Slovenian research agency for funding (grant MR-29397, research programs P1-0021 and P1-0175), prof. dr. Nataša Bukovec for

thermogravimetric analyses and prof. dr. Marjan Marinšek for help with SEM measurements. EPSRC (EP/K007467/1) is thanked for funding support to Andrew M. Beale and I. Lezcano-Gonzalez

7. References

[1] P.G. Smirniotis, W. Zhang, Ind. Eng. Chem. Res. 35 (1996) 3055−3066.

[2] C. Baerlocher, L.B. McCusker, D.H. Olsson, Atlas of Zeolite Framework Types, sixth ed., Elsevier, Amsterdam, 2007.

[3] C. Baerlocher and L.B. McCusker, Database of Zeolite Structures http://www.iza-structure.org/databases/ (accessed 16th August 2016).

[4] R.B. LaPierre, A.C. Rohrman, Jr., J.L. Schlenker, J.D. Wood, M.K. Rubin, W.J. Rohrbaugh, Zeolites 5 (1985) 346−348.

[5] J.C. Trewella, J.L. Schlenker, D.E. Woessner, J.B. Higgins, Zeolites 5 (1985) 130−131.

[6] C.A. Fyfe, H. Gies, G.T. Kokotailo, B. Marler, D.E. Cox, J. Phys. Chem. 94 (1990) 3718−3721.

[7] Y. Kamimura, K. Itabashi, T. Okubo, Micropor. Mesopor. Mater. 147 (2012) 149−156.

[8] Y. Kamimura, K. Iyoki, S.P. Elangovan, K. Itabashi, A. Shimojima, T. Okubo, Micropor. Mesopor. Mater. 163 (2012) 282−290.

[9] M. Kasunič, J. Legiša, A. Meden, N. Zabukovec Logar, A. M. Beale, A. Golobič, Micropor. Mesopor. Mater. 122 (2009) 255−263.

[10] N. Masoumifard, S. Kaliaguine, F. Kleitz, Micropor. Mesopor. Mater. 227 (2016) 258–271.

[11] A. Mitra, C.W. Kirby, Z. Wang, L. Huang, H. Wang, Y. Huang, Y. Yan, Micropor. Mesopor. Mater. 54 (2002) 175−186.

[12] S. Gopal, K. Yoo, P.G. Smirniotis, Micropor. Mesopor. Mater. 49 (2001) 149−156.

[13] A.A. Coelho: TOPAS-Academic, Version 4.1. Coelho Software, 2007, Brisbane, Australia.

[14] C. Paris, N. Martín, J. Martínez-Triguero, M. Moliner, A. Corma, New J. Chem. 40 (2016) 4140–4145.

[15] J. Li, L.-L. Lou, C. Xu, S. Liu, Catal. Commun. 50 (2014) 97–100.

[16] A.S. Araujo, A.O.S. Silva, M.J.B. Souza, A.C.S.L.S. Coutinho, J.M.F.B. Aquino, J.A. Moura, A.M.G. Pedrosa, Adsorption 11 (2005) 159−165.

[17] G. Košová, J. Čejka, Collect. Czech. Chem. Commun. 67 (2002) 1760−1778.

[18] G. Engelhardt, D. Michel: High-Resolution solid-state NMR of Silicates and Zeolites. John Wiley & Sons, Chichester, 1987.

[19] K. Yoo, R. Kashfi, S. Gopal, P.G. Smirniotis, M. Gangoda, R,N. Bose, Micropor. Mesopor. Mater. 60 (2003) 57−68.

[20] W. Zhang, P.G. Smirniotis, M. Gangoda, R.N. Bose, J. Phys. Chem. B104 (2000) 4122−4129.

[21] C.A. Fyfe, H. Strobl, G.T. Kokotailo, C.T. Pasztor, G.E. Barlow, S. Bradley, Zeolites 8 (1988) 132–136.

[22] C.A. Fyfe, Y. Feng, H. Gies, H. Grondey, G.T. Kokotailo, J. Am. Chem. Soc. 112 (1990) 3264–3270.

[23] D.H. Brouwer, J. Magn. Reson. 194 (2008) 136−146.

[24] A-B. Fernandez, A. Marinas, T. Blasco, V. Fornes, A. Corma, J. Catal. 243 (2006) 270-277.

[25] C. Naudin, F. Bonhomme, J.L. Bruneel, L. Ducasse, J. Grondin, J.C. Lassègues, L. Servant, J. Raman Spectroscopy 31 (2000) 979−985.

[26] M. G. O'Brien, A.M. Beale, C.R.A. Catlow, B.M. Weckhuysen, J. Am. Chem. Soc. (2006), 128, 11744−11745.

[27] D.S. Wragg, R.E. Morris, A.W. Burton, Chem. Mater. 20 (2008) 1561−1570.

[28] T. Blasco, A. Corma, J. Martínez-Triguero, J. Catal. 237 (2006) 267–277.

8. Tables

Table 1. The crystal data, collection conditions and refinement parameters for Al-ZSM-12 with TEA.

Crystal data	
Formula	$Si_{41.41}Al_{0.59}O_{84}C_{16}H_{40}N_2$
M_r	2783.63
Crystal system	monoclinic
Space group	*Cc*
a, *b*, *c* (Å)	25.36(2), 15.2124(10), 24.4980(16)
β (°)	108.444(6)
V (Å^3)	8921.8(12)
Z	4
μ (mm^{-1})	0.715
ρ (Mg m^{-3})	2.072
Specimen shape and colour	white powder
Data collection	
Diffractometer	PANalytical X'Pert PRO MPD
Radiation	CuKα1, λ=1.540596 Å
Temperature (K)	293(1)
Tension, current	45 kV, 40 mA
Detector	Full range, 128-channel
Specimen mounting	Flat plate
Data collection mode	Reflection
Scan method	Step
2θ (°)	$2\theta_{min}$ = 5, $2\theta_{max}$ = 86, $2\theta_{step}$ = 0.033
Time per step (s)	500
Refinement data	
R-factors	R_p = 6.950 %, R_p' = 12.367 %, R_{wp} = 9.442 %, R_{wp}' = 15.685 %, R_{exp} =1.928 %, R_{exp}' =3.203 %, R_{Bragg} = 4.066 %

No. of profile points	2459
No. of reflections	3287
No. of structural parameters	6
No. of non-structural parameters	12
Background	Chebyshev polynomial, order 5
Profile	TCHZ-psevdo Voigt profile function (Thompson *et al.*, 1987)

Table 2. The results of Si-Al elemental analysis confirming the higher tendency of Al to incorporate into the framework as compared to Si.

Synthetic ratio n(Si):n(Al)	Elemental analysis results n(Si):n(Al)	Average
80	68	
	69	70
	73	
160	122	
	116	118
	115	

Table 3. The amounts of TEA cations obtained from CHN elemental and thermogravimetric analysis, and the difference between both methods for pure-silica and aluminosilicate frameworks.

	% C	% H	% N
Experimental	6,96	1,66	1,03
Theoretical*	6,90	1,45	1,01
Total amount CHN - experimental [%]		9,65	
Total amount CHN - theoretical [%]*		9,36	
Amount of TEA**		10,16	

	% CHN	% TG
ZSM-12 with TEA	10,45	11,2
Al-ZSM-12 with TEA***	9,65	10,16

*Calculation from expected formula $Si_{41.41}Al_{0.59}O_{84}C_{16}H_{40}N_2$.

**On the basis of mass loss from TG analysis.

***Sample with synthesis Si:Al ratio of 80 (96 h heating at 150 °C).

9. Figure captions

Fig. 1. (a) XRD patterns of Al-ZSM-12 with TEA products with different synthetic Si:Al ratios. Synthesis time and temperature were 96 h and 150 °C, respectively. (b) Formation of superstructural peaks as in pure-silica ZSM-12 with TEA.

Fig. 2. SEM micrographs of a) Al-ZSM-12 with TEA, and b) Pure-silica analogue.

Fig. 3. ^{27}Al MAS NMR spectra of Al-ZSM-12 with TEA (Si:Al = 80, 96 h, 150 °C) and MTEA (Si:Al= 40, 120 h, 150 °C).

Fig. 4. FTIR spectrum of Al-ZSM-12 with TEA recorded at 300 °C under vacuum.

Fig. 5. TGA of Al-ZSM-12 with TEA (synthesis ratio Si:Al = 80).

Fig. 6. Final Rietveld plot obtained for Al-ZSM-12 with TEA (synthesis ratio Si:Al = 80). Red line represents calculated, blue experimental, and grey difference curve. Blue vertical lines represent reflection positions.

Fig. 7. XRD patterns of pure-silica ZSM-12 with MTEA samples synthesized at 150 °C using different synthesis times. For comparison, the pattern of pure-silica ZSM-12 with TEA is given on top. While the crystallinity improves with prolonged heating time, the superstructural peaks (present in pure-silica ZSM-12 with TEA, top) are absent in the pure-silica zeolites synthesised using MTEA, as well as in the aluminosilicate counterpart.

Fig. 8. SEM micrographs of (a) pure-silica and (b) aluminosilicate ZSM-12 with MTEA cations (Si:Al= 40, 120 h, 150 °C).

10. Figures

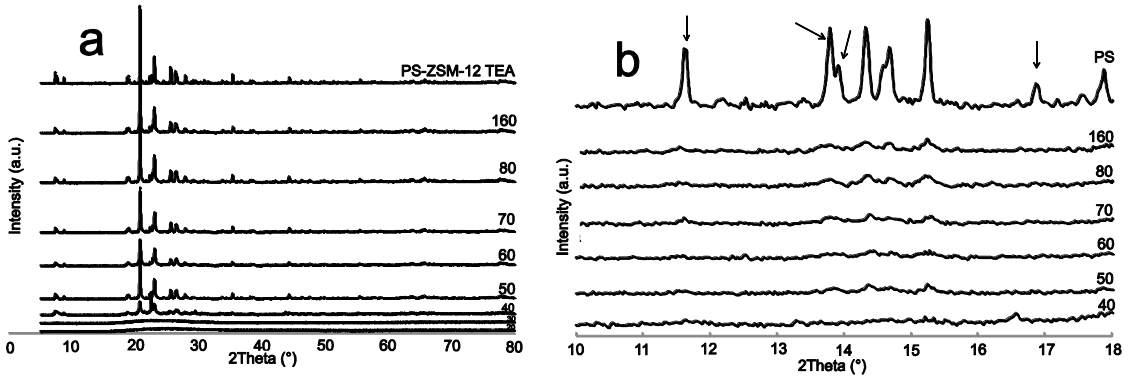

Fig. 1

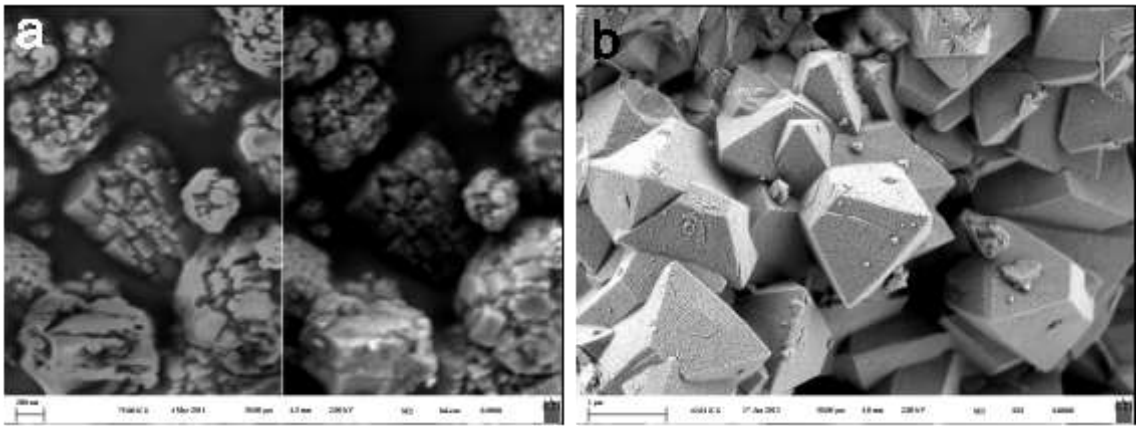

Fig. 2

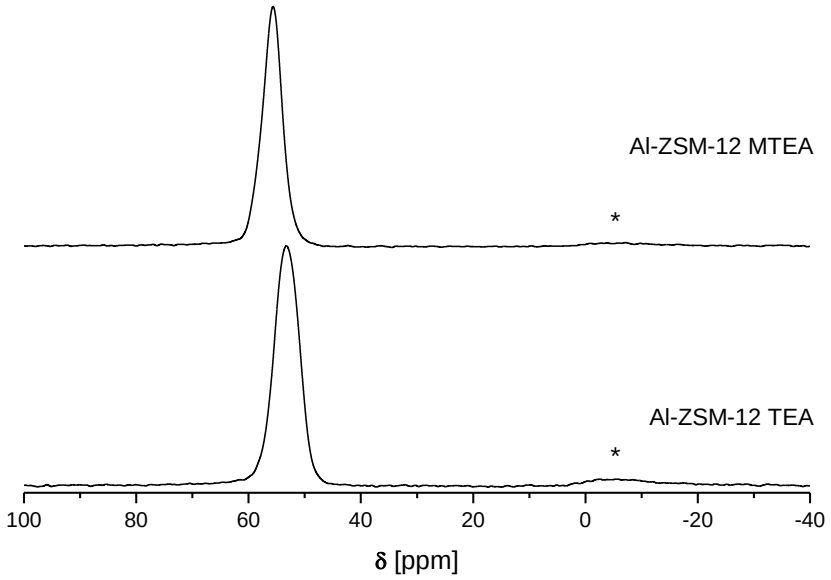
Al-ZSM-12 MTEA
*
Al-ZSM-12 TEA
*
100
80
60
40
20
0
-20
-40
δ [ppm]

Fig. 3

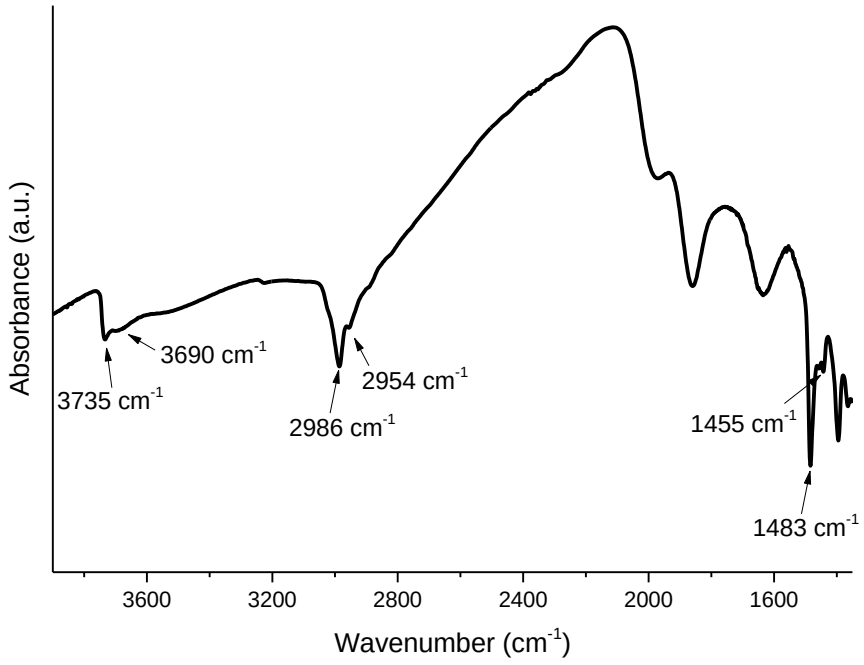
Absorbance (a.u.)
3735 cm-1
3690 cm-1
2986 cm-1
2954 cm-1
1455 cm-1
1483 cm-1
3600
3200
2800
2400
2000
1600
Wavenumber (cm-1)

Fig. 4

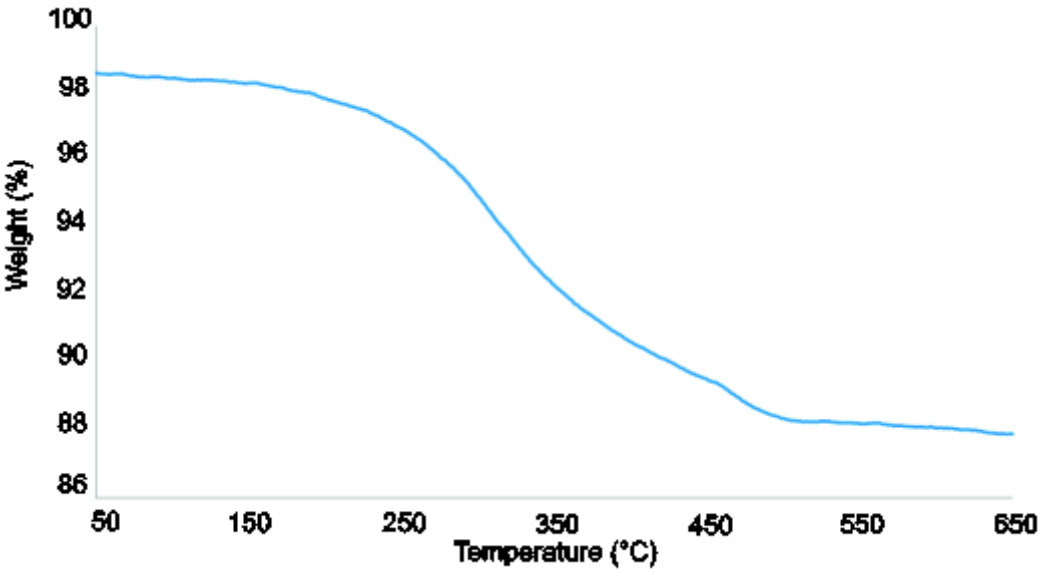
100
98
96
94
92
90
88
86
Weight (%)
50
150
250
350
450
550
650
Temperature (°C)

Fig. 5

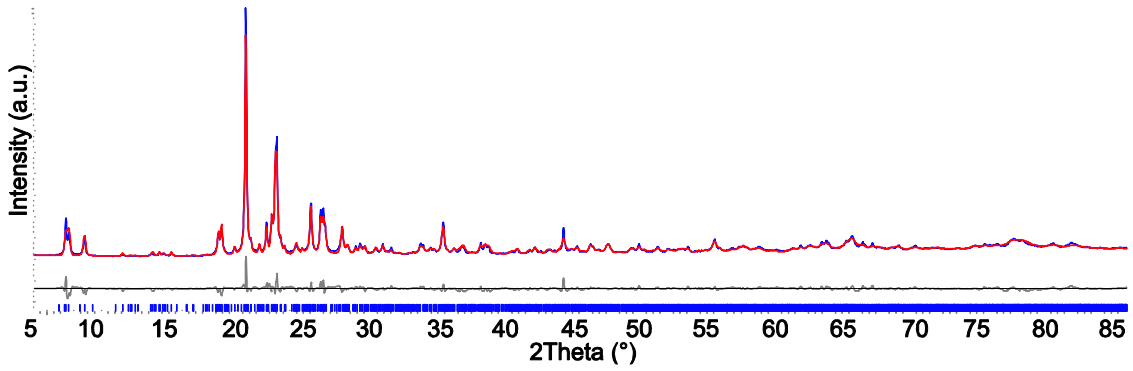
Intensity (a.u.)
5
10
15
20
25
30
35
40
45
50
55
60
65
70
75
80
85
2Theta (°)

Fig. 6

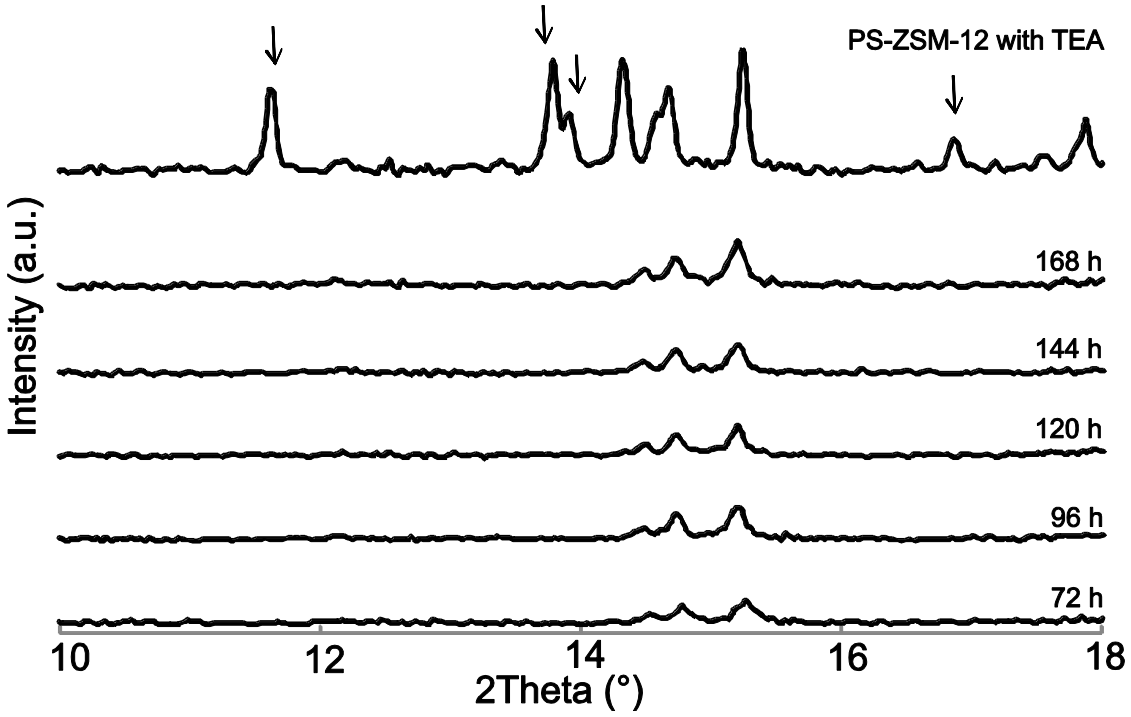
PS-ZSM-12 with TEA
168 h
144 h
120 h
96 h
72 h
Intensity (a.u.)
10
12
14
16
18
2Theta (°)

Fig. 7

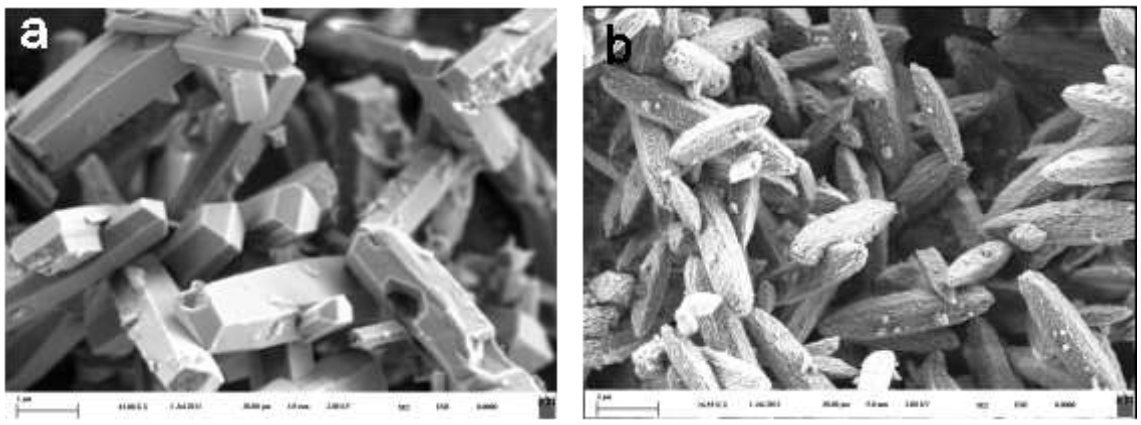
a
b

Fig8